Effects of introducing silica particles on the rheological properties and crystallization behavior of poly(ethylene terephthalate)

Dong Wook Chae · Byoung Chul Kim

Abstract Poly(ethylene terephthalate) (PET)/silica composites were prepared by melt compounding, and their rheological properties and isothermal crystallization were discussed. Introduction of silica particles (0.5–2 wt.%) increased the storage modulus (G') and decreased loss tangent ($\tan\delta$). However, the effect of the particles on rheological properties became negligible at a high frequency more than ca. 70 rad/s. In the Cole–Cole plot, the PET/silica composites showed little deviation from the master curve regardless of the presence of silica particles. The particles increased the relaxation time of PET at particularly low frequency. The isothermal crystallization kinetics of PET/silica was examined using a differential scanning calorimeter (DSC). The half-time of crystallization was decreased with increasing the silica content. The incorporation of silica particles decreased the equilibrium melting temperature by ca. 5.5 °C. In addition, the composites exhibited higher average value of Avrami exponent (2.7–2.9) in comparison with that of pure PET (2.2).

Introduction

Recently, organic–inorganic hybrid is a subject of great interest because it offers unique hybrid properties difficult to obtain from individual components [1]. Synergistic organic–inorganic hybrid materials provide the improved physical properties, such as the mechanical properties, thermal stability, low gas permeability, and chemical reagent resistance [2–5]. In addition, a great versatility of the composites depends upon the many factors including filler size, size distribution, aspect ratio, degree of dispersion and orientation in the matrix, and the adhesion at the filler–matrix interface [6–8]. Various approaches have been taken for the fabrication of the organic–inorganic composites: in situ polymerization [9–11], sol–gel processing [12], and melt compounding [13, 14]. Among them the melt compounding is an economical, simple, and environmentally benign process because it can utilize conventional processing equipment and it does not need solvents. Thus, the direct compounding in a melt state is a promising approach to fabricate polymer particulate systems.

Poly(ethylene terephthalate) (PET) is a semicrystalline engineering polymer and its composites are widely used in the applications such as the automobile, household, and electrical industries. In addition, nano-sized fumed silica has been used in industry as a rheological additive and the useful reinforcement of thermosetting polymer. It serves to improve thermal stability and mechanical properties of the composites. Unusually large specific surface area of the nano-sized particles surely affects the nucleation and crystallization processes of the host polymer. Until now, most of the researches are mainly performed on the clay-incorporated composites. Thus only limited information is available concerning the composites with various inorganic materials even though recently they are used frequently as additives or reinforcement.

D. W. Chae · B. C. Kim (✉)
Division of Applied Chemical & Bio Engineering, Hanyang University, 17 Haengdang, Seongdong, Seoul 133-791, Korea
e-mail: bckim@hanyang.ac.kr

In inorganic particle-filled polymeric systems the rheological studies would be of great help of understanding the polymer chain behavior and determining processing condition. In addition, it is substantially important to study crystallization behaviors because the property of a material depends on the crystallization conditions, especially in the presence of foreign substances. In this work, PET/silica composites in several silica contents were prepared by melt compounding and their rheological properties and isothermal crystallization kinetics were discussed.

Experimental

Preparation of PET/silica composites

PET (intrinsic viscosity = 0.9) was supplied by Hyosung, Inc. (Korea), as a pellet. The PET was vacuum-dried at 90 °C for 24 h prior to melt mixing with silica particles. Silica particles (Sigma Co.), with an average particle size of 109 nm, were incorporated as a fine powder. The PET and silica particles were dry-mixed via tumbling in a bag, and then melt-compounded in an internal mixer (Haake Rheomix 600) for 5 min at 280 °C at a rotor speed of 60 rpm. The loading levels (X) of the composites were 0.5, 1, and 2 wt.%, and they were coded PET-X.

Measurement of physical properties

Field emission scanning electron microscopic (FESEM; JEOL JSM-6330F) observation was carried out on the surface of the composite in sheet, compression-molded in a hot press at 280 °C. Figure 1 shows the FESEM image of the PET composites with 2 wt.% silica. The
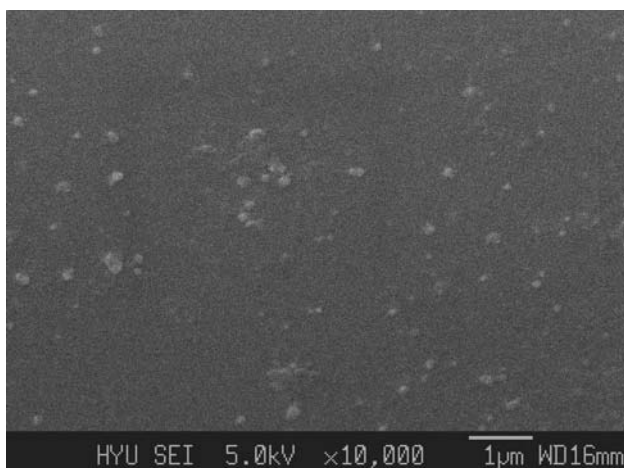
silica particles are dispersed homogeneously in the PET matrix even though an agglomerate of silica is sparsely observed.

The rheological properties of the composites were measured with an Advanced Rheometric Expansion System (ARES: Rheometric Scientific, Inc.) strain-controlled rheometer. Parallel plate geometry with a diameter of 25 mm was employed in an oscillatory mode. The plate gap and strain level were 1 mm and 10%, respectively. The specimen was melted at 280 °C between the parallel plates and the excess flushed-out sample during gap-setting was trimmed off. The specimen was kept for 5 min at the temperature to remove the residual stress. Frequency sweep measurement was conducted over the angular frequency range (ω) of 0.05–500 rad/s at 280 °C in a nitrogen atmosphere.

The thermal properties of PET/silica composites were investigated using differential scanning calorimeter (Perkin-Elmer DSC-7) at a heating rate of 10 °C/min in a nitrogen atmosphere. For isothermal crystallization analysis, the samples were first heated to 280 °C, held in the molten state for 5 min, and then quenched to given crystallization temperatures (T_c): 208, 213, 218, 223, and 228 °C for pure PET, and 213, 218, 223, 228 and 233 °C for the composites.

Results and discussion

The storage modulus (G') of PET and PET/silica composites is plotted against frequency (ω) at 280 °C in Fig. 2. The composites give a little higher value of G'
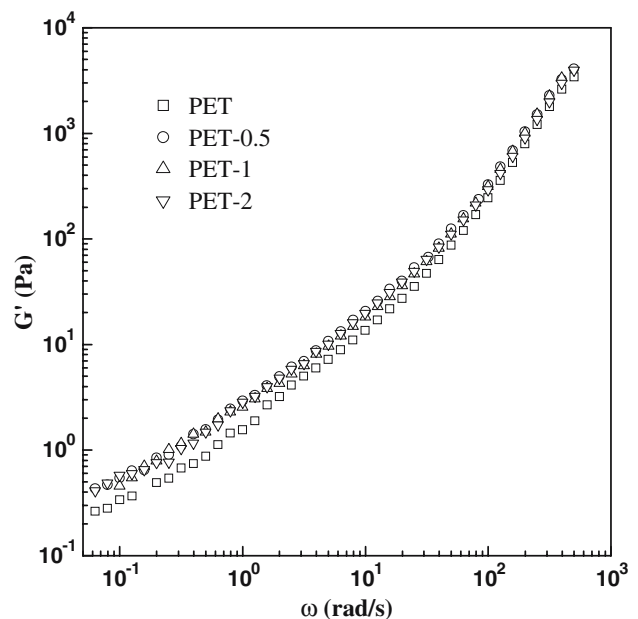

Fig. 1 FESEM images of PET composites with 2 wt.% silica

Fig. 2 G' curve of PET and PET/silica composites at 280 °C

Fig. 3 Tanδ curve of PET and PET/silica composites at 280 °C

Fig. 5 Effects of silica content on λ of PET at three different frequencies
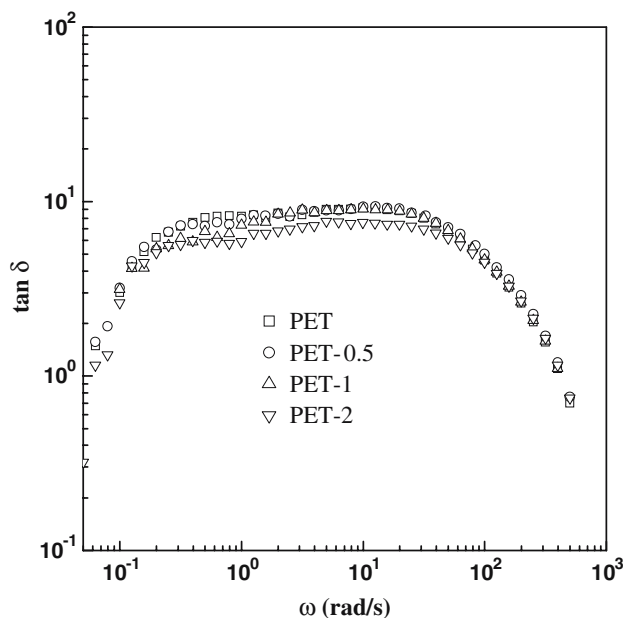
than pure PET in the frequency range less than ca. 70 rad/s. Unusually large specific surface area of the nano-sized particles produces an increase of G' even at such a low silica content. The G' rise upon the presence of the particles is due to the physical association between silica and PET chain. However, all the samples show the almost the same G' value after
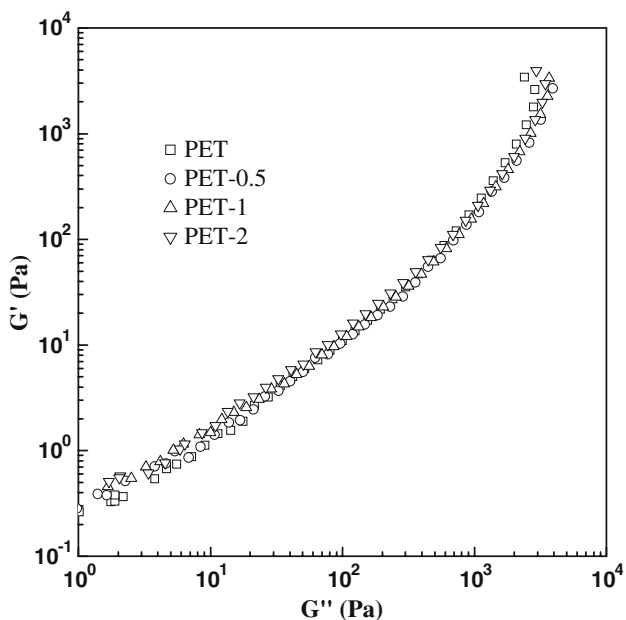

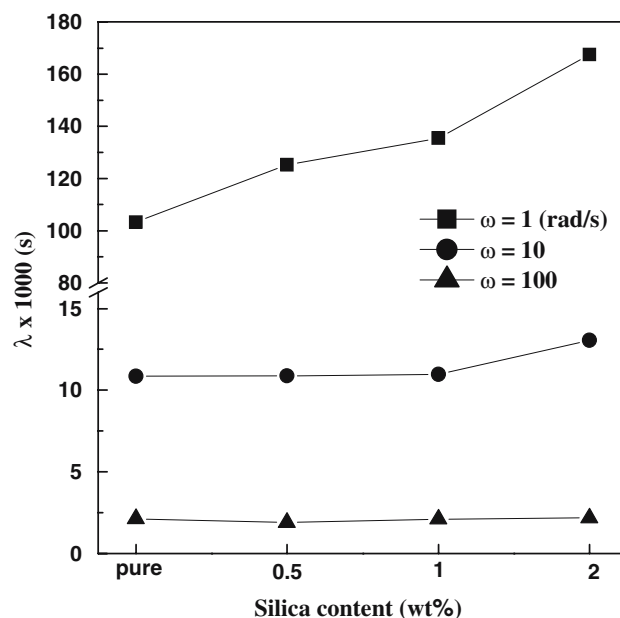Fig. 4 Logarithmic plot of G' versus G'' of PET and PET/silica composites at 280 °C

a frequency of ca. 70 rad/s. This implies that the physical association is not so strong that a role of the particle in the polymer matrix, which limits the chain mobility, becomes negligible under high shear. In addition, the extent of the change in G' does not appear to be sensitive to silica content observed.

Loss tangent (tanδ) is a quantitative measure of solid-like elastic or liquid-like viscose properties of the systems. As shown in Fig. 3, PET-2 shows a lower value of tanδ than the other samples, but almost the same value is observed for all the samples after ca. 70 rad/s. This phenomenon can be inferred that the presence of the particles increases the chain rigidity if the frequency is low enough for the particles to restrict the mobility of the polymer chain.

Figure 4 shows the logarithmic plot of G' versus loss modulus (G'') at 280 °C over the silica content, 0.5–2 wt.%. A so-called Cole–Cole plot gives a single master curve with little scattering of data points. This suggests that the introduction of the particles has little effect on the degree of heterogeneity of the polymeric systems because the physical association between silica and PET chain is not as strong as changing it.

A characteristic relaxation time (λ) of polymeric materials is calculated using an empirical equation substituted by dynamic rheological parameters,

$$\lambda = \frac{G'}{|\eta^*| \times \omega^2} \qquad (1)$$

Fig. 6 Isothermograms of (**a**) PET, (**b**) PET-0.5, (**c**) PET-1 and (**d**) PET-2 at the indicated temperatures
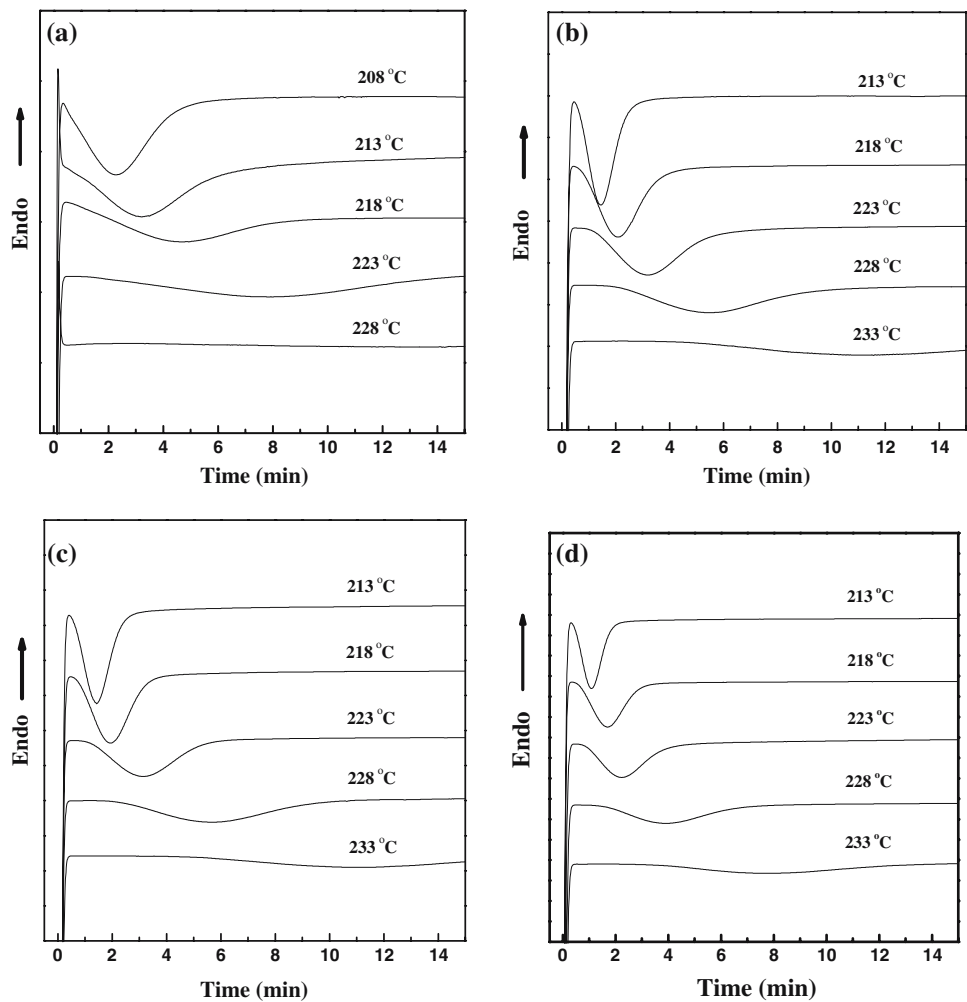
where η^* is the complex viscosity. Figure 5 shows variation of the relaxation time with the silica content at three different frequencies at 280 °C. The introduction of silica particles increases λ of PET notably at 1 rad/s. However, the effects on λ become weak with increasing the frequency. This suggests that the physical association between PET and silica is easily breakable under high shear, as previously mentioned.

Isothermograms of PET and PET/silica composites at the indicated crystallization temperatures are shown in Fig. 6. The crystallization of the composites proceeds slowly at 233 °C, while pure PET dose not show the crystallization behavior at the temperature. The composites display a sharper crystallization peak than pure PET at a corresponding crystallization temperature. In other words, the introduction of silica particles decreases the crystallization time. The relative crystallinity of pure PET and PET-1 is plotted against the crystallization time in Fig. 7(a) and (b), respectively, by following the Avrami treatment. From these curves

the half-time of isothermal crystallization ($t_{1/2}$) is obtained and it is plotted against the crystallization temperature (T_c) in Fig. 8. The $t_{1/2}$ of pure PET is much longer than that of the composites. That is, the introduction of silica particles increases the T_c with their content at the corresponding $t_{1/2}$. This suggests that the crystallization process of the composites is accelerated because of the nucleation effect of silica particles in the systems. In addition, PET-2 presents much lower $t_{1/2}$ than the others at higher T_c. This suggests that the contribution of silica particles to overall crystallization is more notable at a higher temperature, an unfavorable condition for nucleation.

The isothermal crystallization kinetics of the samples is analyzed on the basis of the following Avrami equation,

$$1 - X_t = \exp\left(-kt^n\right) \qquad (2)$$

where X_t is relative crystallinity accumulated at time t, t is the time of crystallization, k is the growth rate

constant, and n is the Avrami exponent. Both k and n depend on the mechanism of the nucleation as well as the crystal growth geometry. Equation (2) can be expressed in the following form by taking logarithms.

$$\log[-\ln(1 - X_t)] = \log k + n \log t \qquad (3)$$

Therefore n and k can be determined by the slope and intersect with y-axis, respectively, in the plot of $\log[-\ln(1 - X_t)]$ versus $\log t$. Figure 9(a) and (b) present the Avrami plots for crystallization of PET and PET-1, respectively. The experimental data are well represented by the Avrami equation in the early stages of the isothermal crystallization. It deviates from the experimental data in the late stages due to the occurrence of secondary crystallization. Table 1 summarizes the values of k and n determined from the
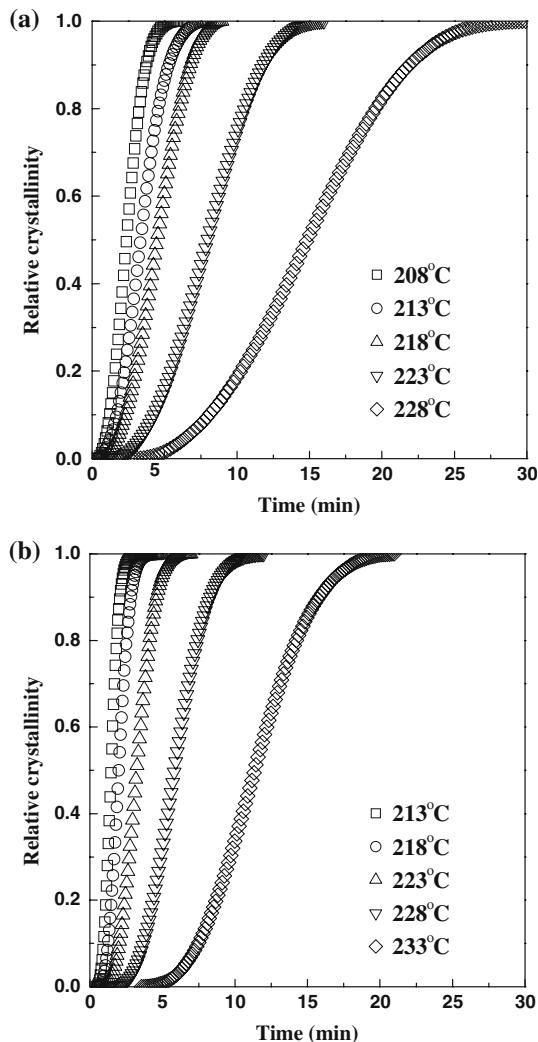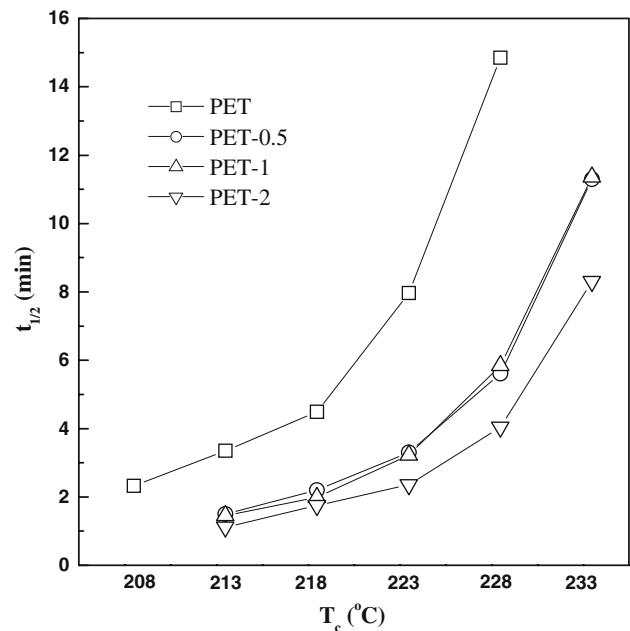

Fig. 8 Temperature dependence of crystallization half time of PET and PET/silica composites

Avrami analysis. The value of n is dependent on the molecular weight, chemical purity, melt condition, and crystallization temperature [15, 16]. The n value of pure PET determined at each crystallization temperature is near average, ca. 2.2 indicating that both the nucleation and the growth mechanism are similar over the crystallization temperature range observed. The composites give a little deviation from average value of

Fig. 7 Development of crystallinity with time during crystallization: (**a**) PET and (**b**) PET-1

Table 1 Isothermal crystallization parameters of PET and PET/silica composites

Sample	T_c (°C)	n	k
PET	208	2.04	140.02×10^{-3}
	213	2.02	56.60×10^{-3}
	218	2.22	27.21×10^{-3}
	223	2.10	11.02×10^{-3}
	228	2.39	1.85×10^{-3}
PET-0.5	213	2.91	492.39×10^{-3}
	218	2.81	140.71×10^{-3}
	223	2.99	25.86×10^{-3}
	228	3.22	3.61×10^{-3}
	233	2.26	10.49×10^{-3}
PET-1	213	2.79	569.39×10^{-3}
	218	2.94	187.10×10^{-3}
	223	3.10	32.92×10^{-3}
	228	2.45	25.34×10^{-3}
	233	2.35	8.90×10^{-3}
PET-2	213	2.79	1195.45×10^{-3}
	218	2.92	213.17×10^{-3}
	223	3.00	96.95×10^{-3}
	228	3.30	10.98×10^{-3}
	233	2.41	15.16×10^{-3}
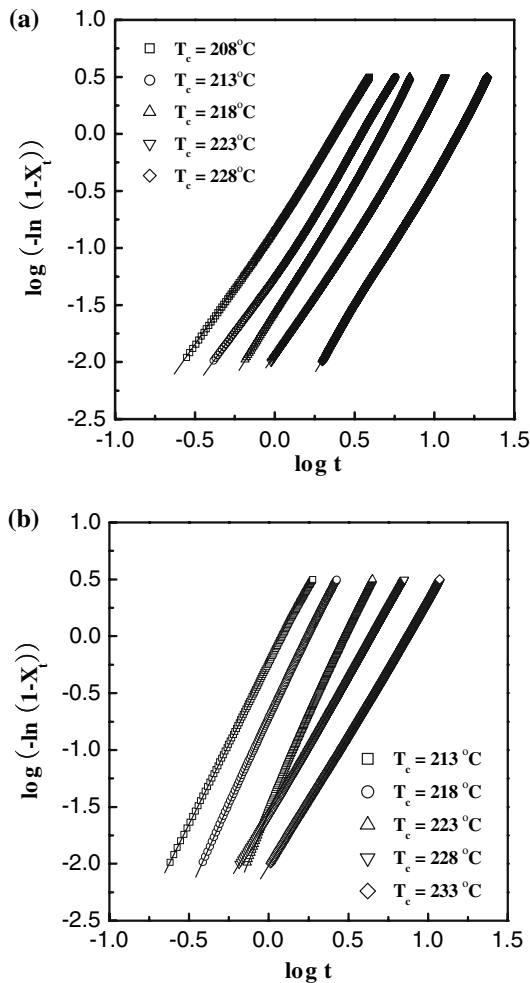
Fig. 9 Avrami plots for isothermal crystallization of (**a**) PET and (**b**) PET-1

Fig. 10 DSC melting thermograms of PET-1, isothermally crystallized at the indicated temperatures

n with the isothermal crystallization temperature. In addition, the composites exhibit the increased average value of n, 2.7–2.9 in comparison with that of pure PET. This suggests that the dimensionality of crystal growth is increased with the incorporation of the particles. The n value of pure PET and its composites in that range means that the crystallization is initiated by heterogeneous nucleation and proceeds with a three-dimensional spherulite growth [17]. The k value is increased with the silica content on the whole, which means that the composites with higher silica content are easier to crystallize. Additionally, the overall rate constant of crystallization is higher at lower T_c.

Figure 10 shows the DSC traces of PET-1 isothermally crystallized at the indicated temperature. The double or triple melting thermograms are observed with isothermal crystallization temperature. Three endotherms are reduced to two when the samples are crystallized over 218 °C as the first and the second
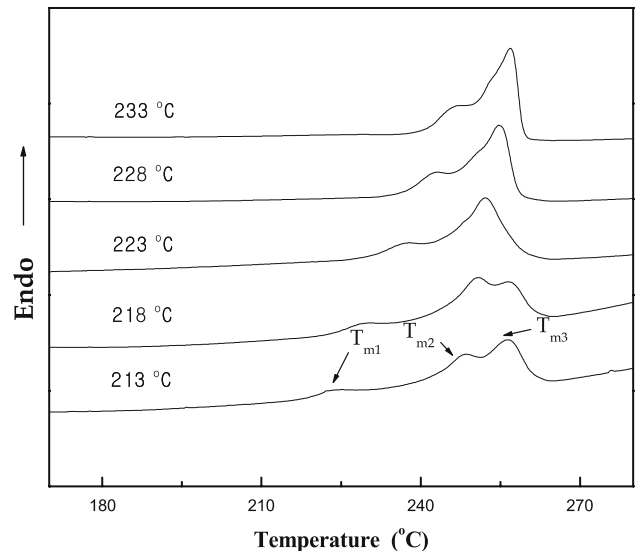
endotherm shift to higher temperatures with increasing the crystallization temperature. The other isothermally crystallized samples show the same tendency of melting behavior. Despite a large number of studies on the multiple behavior of PET, the exact origin of this phenomenon is still under discussion [18, 19]. Zhou and Clough [20] reported the triple-melting behavior of PET: the low temp melting peak (T_{m1}) is related to early melting of secondary crystals, the middle endotherm (T_{m2}), melting of primary crystals, and the high melting endotherm (T_{m3}), recrystallization process taking place upon heating. That is, this multiple melting peaks seem to be caused by the melting of crystallites having different sizes and/or degrees of perfection. In the case of multiple melting behavior, the peak associated with the melting of the crystals formed by primary crystallization is generally used as the T_m value in the Hoffman–Weeks equation. Generally, it is important to measure the equilibrium melting temperature of polymer because T_m depends on the thermal history. The equilibrium melting temperature of the samples can be determined by the Hoffman–Weeks equation, using a plot of T_m versus T_c to $T_m = T_c$,

$$T_m^0 - T_m = \frac{1}{r}(T_m^0 - T_m) \quad (4)$$

where T_m^0 is an equilibrium melting temperature, T_m is the melting temperature crystallized at crystallization temperature, and $1/\gamma$ a slope of $T_m = T_c$. Figure 11 shows the Hoffman–Weeks plot of PET and its composites. The T_m^0 value of the composites ranges
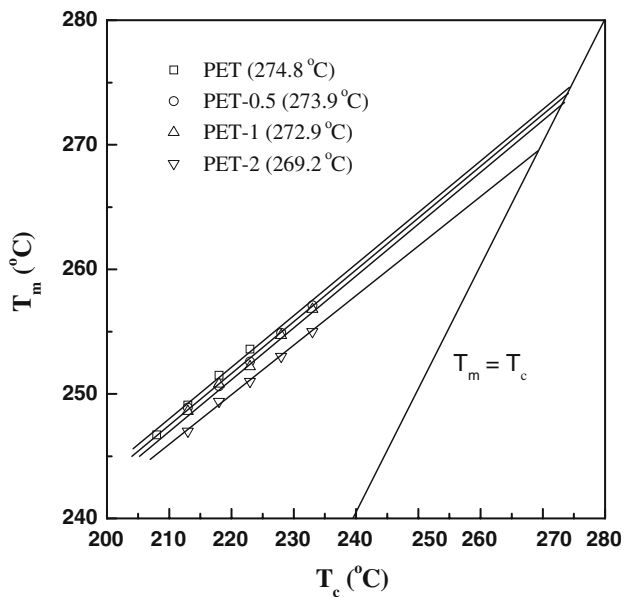
Fig. 11 Hoffman–Weeks plot of isothermally crystallized samples. Equilibrium melting temperature (T_m^0) is indicated

results were of great help of regulating the processing conditions with regard to the real fabrication of the polymeric systems filled with nano-sized particles.

The introduction of silica particles increased the crystallization rate of PET and caused the crystallization to occur at relatively high temperature. This indicated that the silica particle acted as a nucleating agent leading to heterogeneous nucleation. Further, the contribution of silica particles to overall crystallization was more notable at higher crystallization temperature, unfavorable condition for nucleation. In addition, the equilibrium melting temperature was decreased with increasing the silica content, which might be due to heterogeneous nucleation and thereby the formation of small crystal.

from 269.2 to 273.9 °C with silica content, lower than that of PET, 274.8 °C. T_m^0 of the composites is decreased with increasing the loading level. This suggests that the silica particle serves as a nucleating agent leading to heterogeneous nucleation. Thus, the crystal in the presence of silica particles might not undergo large expansion resulting in smaller size than pure PET.

Conclusions

The composites showed a little higher G' than pure PET at the frequency less than ca. 70 rad/s but little difference thereafter. This implied that the incorporation of silica particles appeared to hinder the PET chain mobility to some extent. However, this constraint could be collapsed by applying high frequency, which might result from low particle–polymer interaction. This was verified by the fact that Cole–Cole plot gave a single master curve with little scattering of data points regardless of the presence of the particles. These

References

1. Bicerano J (1998) J Macromol Sci Rev Macromol Chem Phys c38:391
2. Saujanya C, Radhakrishnan S (2001) Polymer 42:6723
3. Yano K, Usuki A, Yurauchi T, Kamigaito O (1993) J Polym Sci Part A: Polym Chem 31:2493
4. Smoug D (1998) Mod Plast 2:28
5. Min ZR, Ming ZQ, Yong XZ, Han ZM, Walter R, Friendrich K (2001) Polymer 42:167
6. Embs FW, Thomas EL, Wung CJ, Prasad PN (1993) Polymer 34:4607
7. Wang Y, Huang JS (1996) J Appl Polym Sci 60:1779
8. Ettlinger M, Ladwig T, Weise A (2000) Prog Org Coat 40:31
9. Yang F, Ou Y, Yu Z (1998) J Appl Polym Sci 69:355
10. Kojima Y, Usuki A, Kawasumi M, Okada A, Kurauchi T, Kamigaito O (1993) J Appl Polym Sci 49:1259
11. Lee DC, Jang LW (1998) J Appl Polym Sci 68:1997
12. Kang ST, Hong SI, Choe CR, Park M, Rim SH, Kim JK (2001) Polymer 42:879
13. Fornes TD, Yoon PJ, Keskkula H, Paul DR (2001) Polymer 42:9929
14. Liu L, Qi Z, Zhu X (1999) J Appl Polym Sci 71:1133
15. Huang JM, Chang FC (2000) J Polym Sci Part B: Polym Phys 38:934
16. Tan S, Su A, Li W, Zhou E (2000) J Polym Sci Part B: Polym Phys 38:53
17. Liu X, Wu Q (2002) Polymer 43:1933
18. Mendellin-Rodriquez FJ, Phillips PJ, Lin JS (1996) Macromolecules 29:7491
19. Qiu G, Tang ZL, Huang NX, Gerking L (1998) J Appl Polym Sci 69:729
20. Zhou C, Clough SB (1988) Polym Eng Sci 28:65